

AD-A272 897



2

ARMY RESEARCH LABORATORY



Microstructural Modeling and Toughening of Si_3N_4 Ceramics for High Temperature Engine Applications

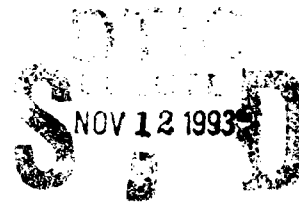
R. L. Yeckley

ARL-CR-62

August 1993

prepared by

Norton Company
Advanced Ceramics
Goddard Road
Northboro, MA 01532-1545



under contract

DAAL04-91-C-0039

93-27531

Approved for public release; distribution unlimited.

88 20 8

The findings in this report are not to be construed as an official Department of the Army position unless so designated by other authorized documents.

Citation of manufacturer's or trade names does not constitute an official endorsement or approval of the use thereof.

Destroy this report when it is no longer needed. Do not return it to the originator.

| REPORT DOCUMENTATION PAGE | | | Form Approved OMB No. 0704-0188 | |
|---|---|--|--|--|
| Public reporting burden for this collection of information is estimated to average 1 hour per response, including the time for reviewing instructions, searching existing data sources, gathering and maintaining the data needed, and completing and reviewing the collection of information. Send comments regarding this burden estimate or any other aspect of this collection of information, including suggestions for reducing this burden, to Washington Headquarters Service, Directorate for Information Operations and Reports, 1215 Jefferson Davis Highway, Suite 1204, Arlington, VA 22202-4302, and to the Office of Management and Budget, Paperwork Reduction Project (0704-0188), Washington, DC 20503. | | | | |
| 1. AGENCY USE ONLY (Leave blank) | | 2. REPORT DATE August 1993 | | 3. REPORT TYPE AND DATES COVERED Final Report 8/30/91 - 10/15/93 |
| 4. TITLE AND SUBTITLE Microstructural Modeling and Toughening of Si ₃ N ₄ Ceramics for High Temperature Engine Applications | | | 5. FUNDING NUMBERS Contract No. DAAL04-91-C-0039 | |
| 6. AUTHOR(S) R. L. Yeckley | | | | |
| 7. PERFORMING ORGANIZATION NAME(S) AND ADDRESS(ES) Norton Company, Advanced Ceramics Goddard Road Northboro, MA 01532-1545 | | | 8. PERFORMING ORGANIZATION REPORT NUMBER | |
| 9. SPONSORING/MONITORING AGENCY NAME(S) AND ADDRESS(ES) U.S. Army Research Laboratory Watertown, MA 02172-0001 ATTN: AMSRL-OP-PR-WT | | | 10. SPONSORING/MONITORING AGENCY REPORT NUMBER ARL-CR-62 | |
| 11. SUPPLEMENTARY NOTES George E. Gazza, COR | | | | |
| 12a. DISTRIBUTION/AVAILABILITY STATEMENT Approved for public release; distribution unlimited. | | | 12b. DISTRIBUTION CODE | |
| 13. ABSTRACT (Maximum 200 words) R-curve behavior was achieved in hot isostatically pressed (HIP) silicon nitride with low additive levels. Two HIP densification processes which produced R-curve in HIP silicon nitride were demonstrated. The first densification process was extended soaks at 1840°C; the second included a pre-HIP sinter step. The strongest R-curve behavior was observed with the rare earth mixture of erbia-samarium, HIPed at 1840°C for 240 minutes. The fracture toughness approached 11 MPa m ^{1/2} at crack lengths of only 600 to 800 microns. Other rare earth combinations were also evaluated. The final microstructure was influenced by the type of rare earths and silica content. The mixed rare earths resulted in a finer and higher aspect ratio microstructure than materials densified with yttria. The development work strongly suggests that a HIP silicon nitride which combines the creep resistance of NT154 type materials with R-curve behavior is possible. | | | | |
| 14. SUBJECT TERMS Silicon nitride, Rare earths, Microstructure, Toughness, Heat treatment, Hot isostatic pressing | | | 15. NUMBER OF PAGES 30 | |
| | | | 16. PRICE CODE | |
| 17. SECURITY CLASSIFICATION OF REPORT Unclassified | 18. SECURITY CLASSIFICATION OF THIS PAGE Unclassified | 19. SECURITY CLASSIFICATION OF ABSTRACT Unclassified | 20. LIMITATION OF ABSTRACT PU | |

5. 10-107-10-240-5500

Standard Form 298, Rev. 3-81
Prescribed by ANSI Std. Z39-18
298-102

Foreword

This research and development work was sponsored by the U.S. Army Materials Technology Laboratory at Watertown, Massachusetts, under Contract No. DAAL04-91-C-0039 for the period 8/30/91 - 10/15/93. Mr. George E. Gazza was the technical point of contact and program monitor.

200 100 100 100

Acquisition For

DTIC
DTIC
DTIC

05.0

A-1

iii

TABLE OF CONTENTS

| | |
|---|-----|
| Foreword | iii |
| 1.0 INTRODUCTION | 1 |
| 2.0 EXPERIMENTAL PROCEDURE | 2 |
| 2.1 Insitu Seeding | 2 |
| 2.2 Composition | 3 |
| 2.3 Mechanical Testing | 4 |
| 2.4 Microstructural Analysis | 4 |
| 3.0 RESULTS AND DISCUSSION | 4 |
| 3.1 Insitu Seeding | 4 |
| 3.1.1 Agglomerates | 4 |
| 3.1.2 β - Si_3N_4 Seeds | 6 |
| 3.2 Composition | 9 |
| 3.3 Thermal Treatments | 12 |
| 3.4 High Temperature Behavior | 18 |
| 4.0 CONCLUSIONS | 21 |
| 5.0 REFERENCES | 22 |

FIGURES

| | | |
|----|---|----|
| 1 | Microstructure after seeding with Si_3N_4 -Er-Y disilicate agglomerates. Highly elongated grains were not observed | 5 |
| 2 | Finer silicon nitride grains were found growing into the disilicate agglomerates of sample DS325 .. | 5 |
| 3 | Fracture toughness decreases with β seed content | 7 |
| 4 | Microstructure BS5 with 5% beta seeds added | 8 |
| 5 | Microstructure of BS20 with 20% beta seeds added | 8 |
| 6 | Strength dependence on silica content for samaria-ytterbia. Room temperature strength decreases with increasing silica content. The error bars are a 95% confidence interval | 9 |
| 7 | Fracture toughness decreases with increasing silica content. The error bars are a 95% confidence interval | 9 |
| 8 | Binary rare earth systems yield increased toughness compared to yttria | 10 |
| 9 | Lognormal plot of grain thickness distribution for four HIP compositions | 10 |
| 10 | Dependence of aspect ratio on grain thickness | 12 |
| 11 | Toughness increases with the frequency of high aspect grains | 12 |
| 12 | Microstructure of Nd50YS after standard HIP | 13 |
| 13 | Microstructure of Nd50YS after 120 minutes at 2150°C | 14 |
| 14 | Although the linear regression deviates from the -1/3 slope, the existence of R-curve is doubtful .. | 14 |
| 15 | Lognormal distribution of grain thickness after 2 hours at 2150°C | 15 |
| 16 | Growth rate is affected by grain boundary composition | 15 |
| 17 | Strength as a function of indent load | 15 |
| 18 | Toughness as a function of crack length for ErSm | 15 |

FIGURES (Cont'd)

| | | |
|----|---|----|
| 19 | The grain distribution of ErSm after an extended time at 1840°C is broader than the other two materials HIPed at 1840°C for 60 minutes | 16 |
| 20 | The ErSm has a high frequency of modest aspect ratio grains greater than 1 micron and fine grains with high aspect ratio | 16 |
| 21 | Dependence of strength of indent load after heat treatments at 1840°C for 4 hours | 17 |
| 22 | Dependence of toughness on crack length | 17 |
| 23 | The compositions with no seeds or 5% seeds showed evidence of R-curve | 18 |
| 24 | The high temperature strength has an apparent minimum at a rare earth to silica ratio of 0.17. The error bars are a 95% confidence interval | 19 |
| 25 | High temperature strength for yttria compositions | 19 |
| 26 | Strain curve for samaria-ytterbia at 1370°C and 200 MPa | 20 |
| 27 | Compressive creep rate at 1370°C and 200 MPa | 20 |
| 28 | Cavitation on two grain boundaries occurs in compressive creep | 21 |

TABLES

| | | |
|---|--|----|
| 1 | Agglomerate types added to silicon nitride with 4% yttria | 3 |
| 2 | Rare earth additive compositions | 3 |
| 3 | Toughness summary for HIP silicon nitride with agglomerate type seeds | 4 |
| 4 | Compositions prepared with β -Si ₃ N ₄ seeds | 7 |
| 5 | Diffraction analysis of binary rare earths after standard HIP cycle | 11 |
| 6 | Summary of compositions heat treated at one of three post-HIP conditions | 13 |

1.0 INTRODUCTION

Hot Isostatically Pressed (HIP) silicon nitrides have the best high temperature fatigue life among silicon nitrides densified by atmospheric sintering, gas pressure sintering (GPS) and HIPing. While the high temperature properties are exceptional, the HIP materials have toughnesses that are not comparable to some GPS silicon nitrides. HIP silicon nitride toughness is independent of crack length. The toughness of HIP silicon nitrides ranges from 5.0 to 6.5 MPa·m^{1/2}. Developing a HIP silicon nitride with R-curve behavior offering improved resistance to machining damage and foreign impact damage would be very beneficial. The objective of this two year program was the development of a HIP silicon nitride with a toughness of 10 MPa·m^{1/2}. The HIP silicon nitride should have 4w/o yttria or the equivalent of another rare earth.

Silicon nitrides exhibiting R-curve appear to have common characteristics. There is a small fraction of grains that have a thickness greater than 1 micron with a high aspect ratio. Several studies have correlated toughness to the frequency of these coarse grains.^{1,2,3} A recent review shows that the toughening contribution associated with large diameter elongated grains is proportional to the grain diameter.¹ Depending on the final grain size distribution, these materials can exhibit high toughness with high strength or high toughness with moderate strength. Typically, these high toughness silicon nitrides are densified with GPS. Several factors during GPS densification enable the formation of the high aspect ratio grains. The rate of grain growth in diffusion controlled mechanisms is shown by :

$$-dr/dt = D (dc/x)$$

where D, dc, and x are, respectively, the diffusion coefficient of materials at grain boundaries, the difference in the solubility between growing and dissolving grains, and the mean separation of two grains. The GPS silicon nitrides complete phase transformation at the intermediate stages of sintering, during which time β silicon nitride growth and pore elimination occur together. The nucleation of large β grains is observed at this stage.¹ The high aspect ratio that develops from α powders during sintering suggests that abnormal grain growth occurs when dc is greater than a critical value. The factors that affect dc are size difference, morphology and phase. These are dependent on temperature. Usually, a portion of the GPS cycle is at temperatures greater than 1850°C. These conditions favor secondary grain growth of the large β nuclei. Abnormal grain growth was observed at high temperatures greater than 1900°C.^{2,3}

In contrast, HIP silicon nitrides have fine grained microstructures resulting in a crack length independent toughness. A recent paper by Sordlett⁵ showed the rapid densification of HIP silicon nitride at temperatures of 1825°C. The silicon nitride reaches densities greater than

90% in 15 minutes. Little grain growth has occurred, and much of the microstructure development takes place in a final densification stage. The opportunity for the formation of large beta nuclei is not available with the current HIP process. In addition, the temperatures may not be sufficient for secondary grain growth.

During the first year of this contract, a number of approaches were screened. The approaches evaluated included seeding, rare earth type, liquid composition, sintering time and sintering temperature. The different techniques all attempted to encourage the formation of beta nuclei or to induce secondary grain growth. The objective was to develop a microstructure that included grains greater than 1 micron in thickness with modest aspect ratios. HIP silicon nitride with R-curve approaching the contract goals was demonstrated.

2.0 EXPERIMENTAL PROCEDURE

2.1 INSITU SEEDING

Two seeding approaches were evaluated. In the first, regions with dissimilar melting points were created. The regions that formed the earliest liquid provided opportunity for preferred growth of the silicon nitride grains. The second approach introduced β - Si_3N_4 seeds into the high α Si_3N_4 powder. The processing was significantly different for the two techniques.

Regions with dissimilar melting points were created by changing the rare earth additive composition within the green body. The melting point was lowered by introducing agglomerates composed of a rare earth binary eutectic within a matrix that had a single rare earth as the densification additive. The agglomerates were formed by spray drying the powders. Before spray drying, the powders were milled for 15 hours in water at 50% solids. The milling media was urethane or nylon coated steel balls. A 3% carbowax plus 0.5% PVA binder was mixed into the slip. The slip was then spray dried. Two types of agglomerate compositions were formed. One type was the eutectic mixture of erbia disilicate-yttria disilicate. The second was a mixture of silicon nitride and the erbia disilicate-yttria disilicate eutectic. The total rare earth content in the second type was 0.0177 moles. The spray dried agglomerates composed of rare earths and silica were air fired between 700°C and 1300°C. The agglomerates were air fired between 500°C and 900°C if the composition included silicon nitride. Calcining the screened agglomerates prevented their breakdown during the subsequent forming process. Two size classifications were prepared by screening the air fired agglomerates. The spray dry agglomerates were screened to size fractions of -100/+200 and -325 mesh. The agglomerates were dispersed in a powder with the composition of 94w/o silicon nitride-4w/o yttria-2w/o silica. The tile were prepared by slip casting. The agglomerate size fraction and weight percent added is shown in Table 1. The tile were then heat treated at 1700°C for 30 minutes or 1700°C for 90 minutes to allow beta silicon nitride grain

Table 1. Agglomerate types added to silicon nitride with 4% yttria.

| Batch ID | Type | Size | wt % |
|----------|--|---------|------|
| DS100 | Er-Y disilicate eutectic | 100/200 | 5 |
| SN325 | Si ₃ N ₄ with Er-Y disilicate eutectic | 325 | 5 |
| SN100 | Si ₃ N ₄ with Er-Y disilicate eutectic | 100/200 | 30 |
| DS325 | Er-Y disilicate eutectic | 325 | 30 |

growth in the agglomerates. This temperature is above the erbia-yttria disilicate eutectic, but below the yttria disilicate melting point. After the heat treatment, the tile were HIPed to full density.

The other seeding approach used β -Si₃N₄ particles as seeds. The β -Si₃N₄ seeds were fabricated by heating silicon nitride powder with 2% of the rare earth to 1840°C under 300 psi of nitrogen for 4 hours. The seeds were then milled for 24 hours and dried. The milled seeds were added to standard compositions. These were milled for 15 hours in water and spray dried. Tile were pressed and isopressed at 30 ksi. The tile were air fired at 600°C for 2 hours to remove the binder. The tile were then ready for densification treatments.

2.2 COMPOSITION

The effect of the rare earth to silica ratio on the mechanical properties were studied. The rare earth to silica molar ratio was varied in the range of 0.3 to 0.1. The rare earth was either yttria or the combination of ytterbia - samaria. In addition, the effect of binary rare earths on the toughness and microstructure were studied. These rare earth systems are shown in Table 2. The rare earth content is 0.0177 moles per 100 grams of powder, which is equivalent to 4w/o yttria.

The silicon nitride, rare earths and silica were milled for 15 hours at 60% solids in water. The milling media was polyurethane or nylon coated steel balls. The mixes were screened through a 20 micron filter, then spray dried. Three inch square tile were prepared from these batches by CIPing at 30 ksi. The tile were air fired to remove the binder prior to HIPing.

Table 2. Rare earth additive compositions.(w/o)

| | Er2O3 | La2O3 | Sm2O3 | Yb2O3 | Nd2O3 | Y2O3 | SiO2 |
|---------|-------|-------|-------|-------|-------|------|------|
| Er50YS | 3.44 | | | | | 1.97 | 2.13 |
| Er59YS | 4.00 | | | | | 1.64 | 2.13 |
| La40YbS | 2.31 | | | 4.19 | | | 2.13 |
| La35YS | | 2.02 | | 2.6 | | | 2.13 |
| Nd50YbS | | | | 3.49 | 2.98 | | 2.13 |
| Nd50Y | | 2.00 | | 2.98 | | | |
| SMYbS | | | 3.09 | 3.49 | | | 2.13 |
| SmYb | | | 3.09 | 3.49 | | | |
| Er50SmS | 3.44 | | 3.08 | | | | 2.13 |
| ErSm | 3.44 | | 3.08 | | | | |
| NdYb | | | | 3.49 | 2.98 | | |

2.3 MECHANICAL TESTING

All strength testing was done on a 4-point quarter-point fixture with an outer span of 40 mm. Toughness was determined by the indentation fracture method. The flexure bar size was 3 mm x 4 mm x 50 mm, or 3 mm x 4 mm x 25 mm. Fracture toughness was determined by the indentation-strength technique. The indent load was 10 kg. Unless specifically noted in the document all toughness results are from the above test technique. The presence of R-curve behavior was determined by the dependence of strength on indent load. The indent load range was 2.5 to 50 kilograms.

Compressive creep specimens were 6.7 mm x 25.4 mm cylinders. The cylinders were loaded between SiC rods. Four silicon nitride flags were cantilevered on the cylinders. The distance between these flags was measured by a non-contact laser extensometer system. 2.4 Microstructure Analysis

2.4 MICROSTRUCTURAL ANALYSIS

The microstructural analysis was done by polishing and then etching the samples in molten KOH. Micrographs were taken at 2.5 KX, 5KX and 10 KX. Grain thickness was measured by drawing four to six lines across the micrographs. The shortest dimension of any hexagonal or rectangular shaped grains intercepted by the lines was measured. The aspect ratio was estimated from 2.5X micrographs. Four lines were drawn across the micrographs. The thickness and length were recorded for each rectangular grain touching a line. This resulted in an estimate of the apparent aspect ratio distribution.

3.0 RESULTS AND DISCUSSION

3.1 INSITU SEEDING

3.1.1 Agglomerates - Neither agglomerate type increased the grain aspect ratio, and the presence of the agglomerates reduced the fracture toughness of HIPed silicon nitride. The fracture toughness data is

Table 3. Toughness summary for HIP silicon nitride with agglomerate type seeds.

| Batch ID | 1700°C 90 min | | 1700°C 30 min | |
|----------|---------------------------|----------|---------------------------|----------|
| | Mean | st. dev. | Mean | st. dev. |
| DS100 | 5.40 MPa·m ^{1/2} | 0.14 | 3.93 MPa·m ^{1/2} | 0.12 |
| SN325 | 3.96 | 0.13 | | |
| SN100 | 4.11 | 0.11 | | |
| DS325 | 4.12 | 0.09 | | |

summarized in Table 3. A similar yttria composition without the inclusion of seeds had a typical fracture toughness range of 5.5 to 6.5 MPa·m^{1/2}.

The agglomerates' effect on grain development may not have been detected by toughness measurement. The coarse agglomerates introduced into the casting slip may segregate during forming. An inhomogeneous distribution of the agglomerates could affect the measured toughness. This did not appear to be an issue, based on the uniform glass pocket distribution observed in the polished sections. The microstructures around the agglomerates were examined for evidence of enhanced grain growth. The presence of coarser grains would suggest that modified processing to change the grain distribution may improve the measured toughness.

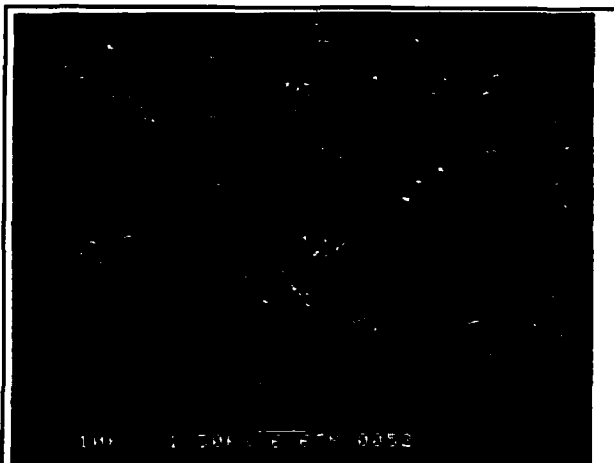


Figure 1. Microstructure after seeding with Si_3N_4 -Er-Y disilicate agglomerates. Highly elongated grains were not observed.

sample. Evidence of elongated grain growth was not observed with agglomerates composed of erbia-yttria-silicon nitride.

The disilicate seeds left glass pockets behind after HIPing. These pockets were visible in polished sections. Figure 2 shows the microstructure around the glass pocket for DS325. This silicon nitride had 30 w/o of the agglomerates added. The total rare earth content was significantly higher than the 0.0177 moles per 100 gms of powder. The high frequency of agglomerates was added to

Figure 1 is an etched micrograph from batch SN100. SN100 was the mixture of silicon nitride and rare earth plus silica. The liquid content of the agglomerate was equal to the surrounding matrix. The etched microstructure shows 5 to 10 micron wide areas of high glass content. Normally, the intergranular glass is distributed uniformly. The silicon nitride grain size distribution was uniform throughout the

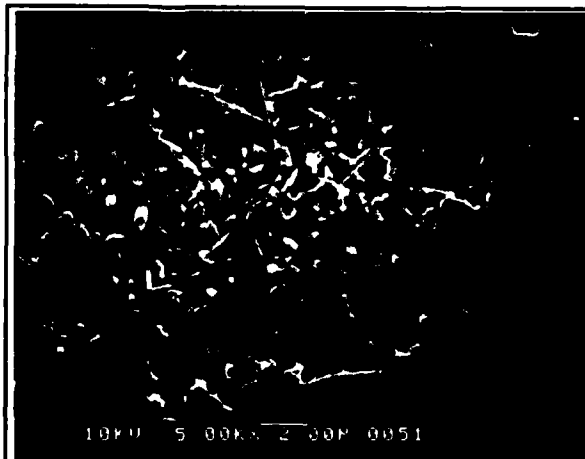


Figure 2. Finer silicon nitride grains were found growing into the disilicate agglomerates of sample DS325.

determine if any effect on grain growth could be observed. Examination of the microstructures showed that refinement of the grains was observed in the regions of the agglomerates. Exaggerated grain growth was not observed, and the presence of the glass pockets would degrade the mechanical performance of the material.

An additional batch was prepared in which 4 w/o of a rare earth agglomerate was added to silicon nitride powder. The agglomerate was the only sintering additive used. The agglomerates were -325 mesh, and the agglomerate composition was $\text{Nd}_2\text{O}_3\text{-2SiO}_2$. This modification was attempted because the earlier trials had additive in both the agglomerate and the matrix. In this trial, the $\text{Nd}_2\text{O}_3\text{-2SiO}_2$ represents all the densification additive. The driving force to distribute the liquid and eliminate the porosity should be stronger than in the previous trials. The material was fully dense after HIPing. Agglomerate remnants were observed on the polished cross section. These glass pockets did have some silicon nitride growing into the pocket, but the glass regions would result in poor mechanical properties. The toughness of this material was only $3.99 \text{ MPa}\cdot\text{m}^{1/2}$.

The original concept was that grain growth would occur at the localized regions of liquid. The liquid regions would be formed by regions which were composed of densification additives that would melt at lower temperatures than would the surrounding matrix. In the rare earth systems, the maximum temperature difference was only 100°C . The eutectic liquid formed at temperatures of 1650°C to 1700°C . Since the compositions were to have only the equivalent of 4 w/o yttria, the amount of liquid was small. Under these conditions, silicon nitride solubility would be small, and diffusion would be slow. Little grain growth would be expected at the 1700°C pre-HIP sinter step. Time was not provided during the subsequent HIP cycle at temperatures below 1800°C . Below 1800°C , densification rates are very slow. Slow densification increase reaction problems with the glass encapsulant. Therefore, a temperature was reached where liquid would be present throughout the compact. No time is provided for grain growth in local regions of a compact. In addition, particle rearrangement occurs rapidly under 30 ksi and closed porosity is reached rapidly.⁵ Since the liquid composition of the agglomerates is basically the intergranular composition, there is no driving force for elimination of the liquid-filled pores. In liquid phase HIP alumina, 100 to 150 micron voids were shown to fill with liquid during HIP, but were not eliminated.⁶ The behavior of the agglomerates in the HIP silicon nitride was very similar. The incorporation of agglomerates reduced toughness, and did not enhance grain elongation.

3.1.2 $\beta\text{-Si}_3\text{N}_4$ Seeds - Sintered silicon nitride with a fairly high amount of sintering additive reportedly increased toughness with the addition of β seeds.⁷ The seeds were prepared by blending $\alpha\text{-Si}_3\text{N}_4$ powder

with 2% yttria. The powder blend was then heated to 1750°C for 4 hours, converting the powder to β -Si₃N₄ whiskers. The β -Si₃N₄ was then milled. The milled powders were then used as seeds in a silicon nitride composition. The densification of this material was rapid, and at temperatures similar to the HIPed silicon nitride. A similar approach may increase the elongation of HIPed silicon nitride.

The β -Si₃N₄ seeds produced in this work had an average particle size of less than 1 micron. These were added to silicon nitride with sufficient yttria to bring the total to 4% yttria. Batches with 5, 10 and 20 weight percent of beta seeds were prepared. In addition, compositions with other rare earths were prepared. The compositions with β seeds are listed in Table 4.

Table 4 Compositions prepared with β -Si₃N₄ seeds.

| Batch | w/o Seeds | Additive |
|---------|-----------|---|
| BS5 | 5 | 4w/o yttria |
| BS10 | 10 | 4w/o yttria |
| BS20 | 20 | 4w/o yttria |
| SmYbBS5 | 5 | 2.94 w/o Sm ₂ O ₃ , 3.32 w/o Yb ₂ O ₃ |
| YbBS5 | 5 | 1.74 w/o Yb ₂ O ₃ |
| SmBS5 | 5 | 1.5 w/o Sm ₂ O ₃ |

The yttria compositions with beta seeds had a toughness independent of crack length. The fracture toughness was lower than the standard monolithic material at all beta seed levels. Figure 3 shows the dependence of fracture toughness on the beta seed content. The toughness decreases with increasing β content, up to approximately 10 w/o seeds. The toughness appears to reach a minimum of 3.0 MPa·m^{1/2}. This is similar to silicon nitride toughness with low amounts of additives. These microstructures have low aspect ratios.

Figure 4 and Figure 5 show the reduced aspect ratio of the microstructure as the seed content increases from 5 to 20 w/o.

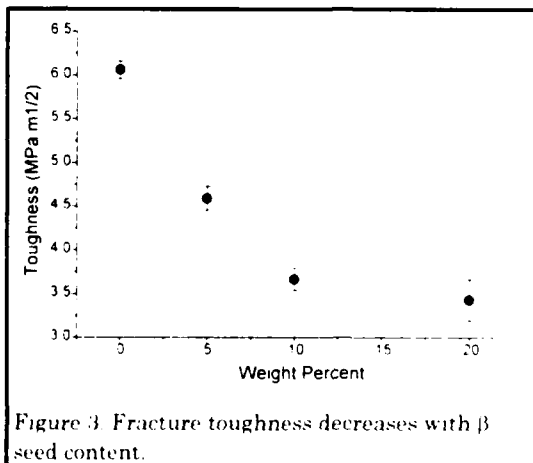


Figure 3 Fracture toughness decreases with β seed content.



Figure 4. Microstructure BS5 with 5% beta seeds added

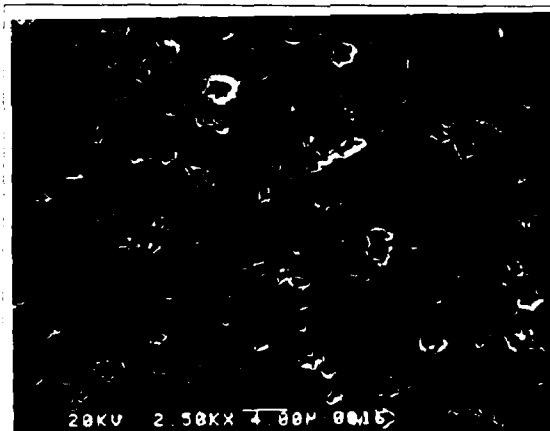


Figure 5. Microstructure BS20 with 20% beta seeds added

3.2 COMPOSITION

The initial composition work began in parallel with the agglomerate seeding task. The use of agglomerates to encourage grain growth might be affected by the liquid composition within the agglomerate. Diffusion and/or solubility may be enhanced

by controlling the liquid composition. Changes in these parameters could change the final grain distribution. Specifically, the compositional task started by examining the role of the rare earth to silica ratio on the final properties. The optimum composition would have been

incorporated into seed preparation. The effect of the rare earth to silica ratio was investigated for two densification systems. Yttria was used as one densification additive. An equimolar mixture of ytterbia and samaria was the second additive system. The rare earth to silica ratio was varied from 0.1 to 0.35. Room temperature strength as a function of rare earth content is plotted in Figure 6. Strength decreases

with increasing silica content. A similar trend is observed with fracture toughness in Figure 7. The mixed rare earth had higher fracture toughness than yttria alone.

The effect of rare earth on grain morphology and fracture toughness was expanded. The compositions are summarized in Table 2. Some densification additives included additional silica. The silica on the nitride surfaces plus the added silica, was sufficient to make the rare earth to silica molar ratio

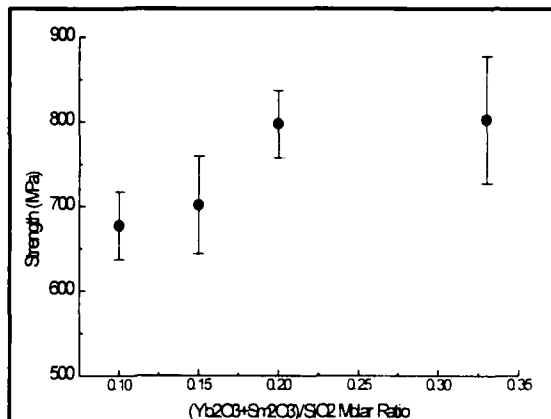


Figure 6. Strength dependence on silica content for samaria-ytterbia. Room Temperature strength decreases with increasing silica content. The error bars are a 95 % confidence interval.

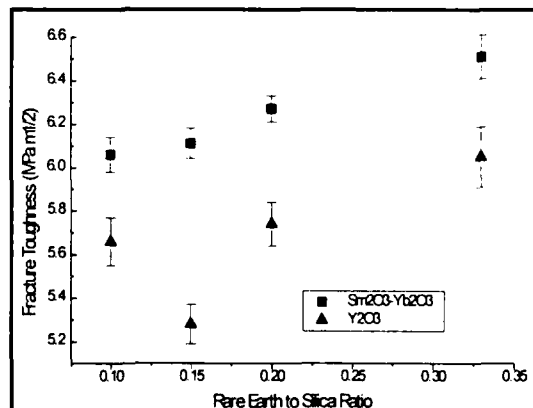


Figure 7. Fracture toughness decreases with increasing silica content. The error bars are a 95% confidence interval.

earth to silica molar ratio equal to the rare earth disilicate. Data for all the systems are not available because numerous tile were not dense due to encapsulation failure. Additional tile were not HIPed, because the binary rare earths may offer 10 to 30% improvements in toughness, but would not achieve the program goals alone.

The fracture toughnesses are compared in Figure 8. The compositions with an asterisk are the average of two HIP runs. The compositions plotted in Figure 8 were prepared with added silica. The binary rare earth systems have slightly higher toughnesses than do silicon nitride HIPed with yttria and silica. Other single rare earth oxides were not prepared.

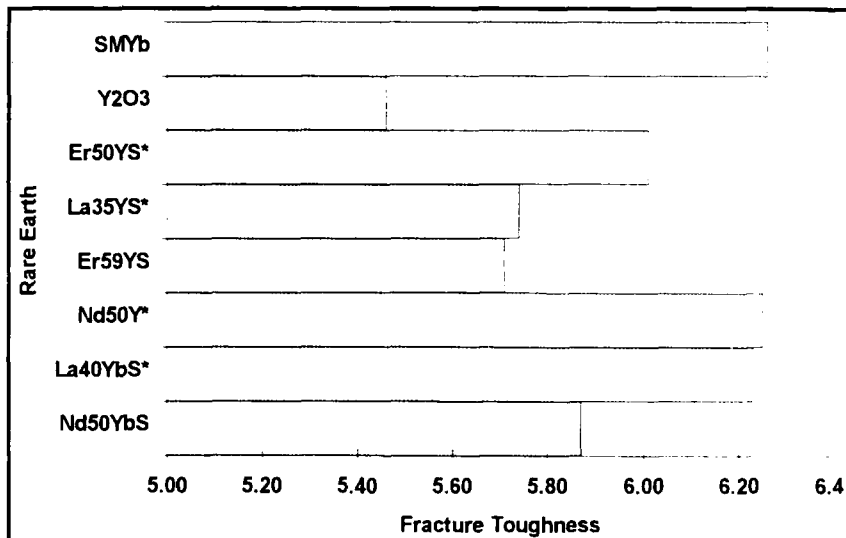


Figure 8 Binary rare earth systems yield increased toughness compared to yttria.

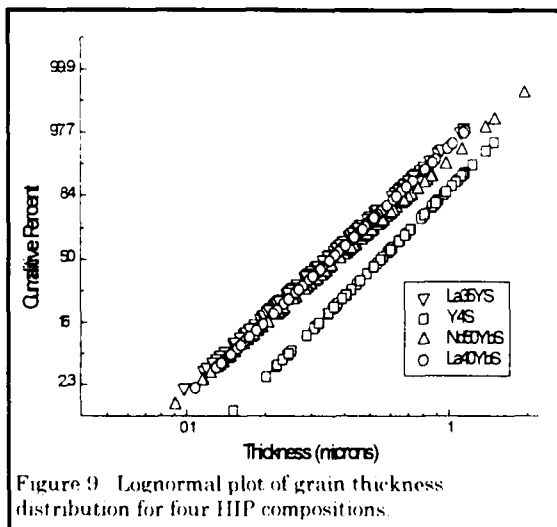


Figure 9 Lognormal plot of grain thickness distribution for four HIP compositions.

The microstructures were characterized and correlated to the fracture toughness. The grain thickness was measured from 10KX micrographs. Figure 9 is a lognormal plot of the grain thickness distributions. The linear relationship of the data is evidence that the lognormal distribution is a good description of the

distribution. The similarity of the slopes indicates that the grain thickness distribution width is similar. The binary rare earth systems yielded a smaller grain size than the yttria. The starting particle size was equivalent, and would not account for differences in the final grain size. Some explanation is found by looking at the phases present after HIPing. The α - Si_3N_4 content for the mixed rare earths is shown in Table 5. The yttria composition had 11% α - Si_3N_4 after HIPing. Less transformation will result in the finer grain size. In Figure 9, the coarse end of all distributions is very similar. The binary rare earths have a finer tail caused by the fine β and α grains that have not yet reprecipitated on the larger β grains, although it is not clear by what mechanism the transformation rate is reduced in the presence of the binary rare earth systems. The rare earths forming the mixture did not seem to affect the grain size after the standard HIP cycle. The extent of the α to β transformation was also similar.

Table 5. Diffraction analysis of binary rare earths after standard HIP cycle.

| | oxy | alpha | beta | phase | rel int |
|---------|-------|--------|--------|---|---------|
| Nd50YbS | 3.72% | 30.84% | 65.44% | Nd ₂ Si ₂ O ₇ alpha | 3.3 |
| La40YbS | 2.24% | 33.23% | 64.53% | | |
| Nd50Y | 2.50% | 27.29% | 70.21% | Y ₂ Si ₂ O ₇ | 2.3 |
| Er59YS | 2.13% | 30.38% | 67.48% | | |
| La35YS | 2.04% | 35.02% | 62.94% | | |
| Er50YS | 2.20% | 26.74% | 71.06% | Y ₂ Si ₂ O ₇ | 2.5 |

The grain thickness of the HIP silicon nitrides with binary rare earths are very similar and finer than the yttria composition, but all the materials are relatively fine grained with a very small percentage of grains greater than one micron. Current theories on toughening in silicon nitride indicate that crack bridging is a factor primarily with grain thicknesses of over 1 micron. Since these HIP materials are very fine grained, the increased toughnesses are probably due to crack deflection mechanisms. Toughness changes should depend on differences in the aspect ratio or frequency of elongated grains in the mixed rare earth systems. The estimated aspect ratios are plotted as a function of grain thickness for two binary rare earth systems in Figure 10. The aspect ratio appears to reach an asymptotic value of 4 as the diameter increases. The same value was suggested by Mitomo¹ as the equilibrium β aspect ratio. The highest aspect ratios are found for grains less than 0.6 microns. As the thickness increases, the maximum aspect ratio decreases. This trend was observed for all the HIPed compositions. Comparison of the aspect ratio between materials was not considered, because of the uncertainty of measuring the aspect ratio from a 2-D image and the small sample size for each material. The toughening mechanism for small diameter, high aspect ratio grains is expected to be crack deflection. In crack

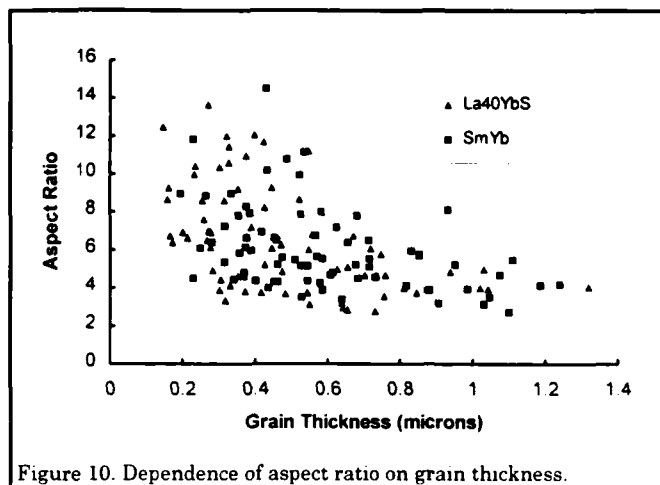


Figure 10. Dependence of aspect ratio on grain thickness.

deflection models⁸ toughness is dependent on the frequency of the high aspect ratio grains.

The dependence of aspect frequency on toughness was evaluated. A linear density of grains with an aspect greater than four was determined for each sample. The linear density is defined as the number of grains with an aspect greater than 4, divided by the total line length traversed across the micrographs. Figure 11 shows an increasing toughness with a higher linear density for the different rare earth systems. Silicon nitride with two rare earths had a higher frequency of high aspect grains than yttria. The toughness range of 6.0 to 6.5 $\text{MPa}\cdot\text{m}^{1/2}$ is very good for a HIP silicon nitride, but a crack deflection mechanism in HIP silicon nitride may not be able to provide toughness approaching or exceeding 8 $\text{MPa}\cdot\text{m}^{1/2}$. Toughness exceeding 8 $\text{MPa}\cdot\text{m}^{1/2}$ would probably require increased contribution from crack bridging mechanisms. This should lead to R-curve behavior in the HIP silicon nitride. Experimental thermal treatments that might favor the development of high aspect ratio grains with thicknesses of one micron or greater were then conducted.

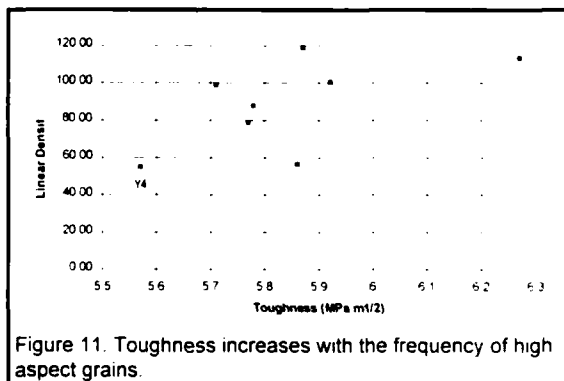


Figure 11. Toughness increases with the frequency of high aspect grains.

3.3 THERMAL TREATMENTS

Typically, the high toughness silicon nitrides have large, high aspect ratio grains. The development of these grains is due to secondary grain growth from large β nuclei at high temperatures. The pre-HIP sinter conditions did not form large beta grains because of the low temperatures and short times. The insitu seeding with agglomerates failed to increase the silicon nitride aspect ratio. Also, the HIP temperature may be too low for secondary grain growth if large beta nuclei were present. Thermal treatments examined two factors with the HIP silicon nitride that may encourage the development of elongated grains: first, increased temperature that would increase diffusion rates and may allow larger grains already present in the matrix to grow, consuming smaller grains; second, the use of high temperatures in a pre-HIP sinter cycle that would form large beta crystals. Then, during a standard HIP cycle, the large beta grains would grow rapidly, at the expense of smaller grains surrounding them.

The compositions subjected to a post-HIP heat treatment are listed in Table 6. These tile had already been HIPed to full density. Since the tile were dense, the post-HIP treatment was done without glass encapsulation. The tile were covered with silicon nitride powder. These trials would determine the extent of grain coarsening and the potential effects on toughness during high temperature HIPing. Figure 12 and Figure 13 show the microstructural coarsening that occurred during the post-HIP treatment at 2150°C for Nd50YS.

Table 6. Summary of compositions heat treated at one of three post-HIP conditions

| Conditions | NdYb | YbBS | ErSm | Er50SmS | Er59YS | Er50YS | Nd50YS | Sm | Nd50YbS | Y4 |
|--------------------------------|------|------|------|---------|--------|--------|--------|----|---------|----|
| 2150°C, 30 ksi, 120 minutes | | | | | ✓ | ✓ | ✓ | | ✓ | ✓ |
| 2000°C 30 ksi, 120 minutes | | | | | ✓ | ✓ | ✓ | | | |
| 1840°C, 15 ksi 1 hours | ✓ | ✓ | ✓ | ✓ | | | | ✓ | | |

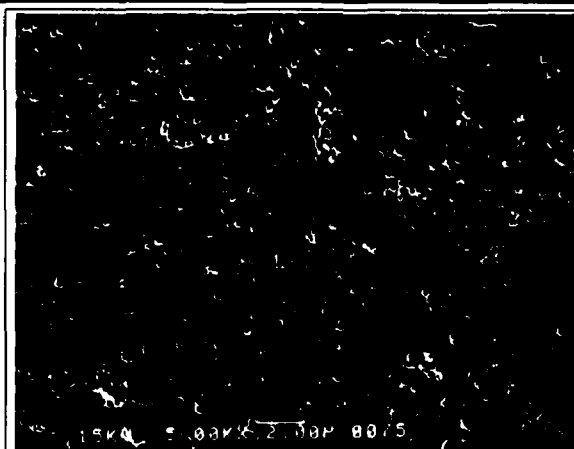


Figure 12. Microstructure of Nd50YS after standard HIP.

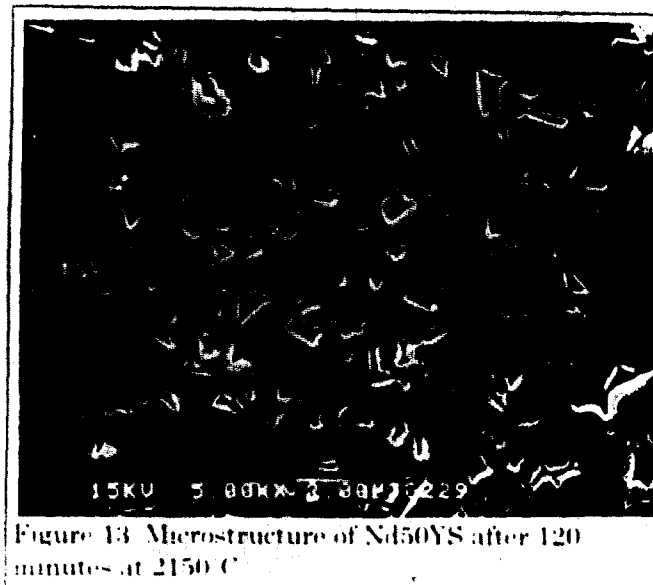


Figure 13 Microstructure of Nd50YS after 120 minutes at 2150 °C

None of the HIP silicon nitrides with binary rare earths exhibited R curve behavior after HIPing at 2150 °C or 2000 °C.

Figure 14 is a plot of the dependence of fracture strength on indent load for HIP silicon nitride with yttria after 2150 °C post-HIP. The -0.15 slope from linear regression deviates significantly from the -1/3 slope indicating the material exhibits R curve behavior; however, the data scatter was large. In addition, the strength of the

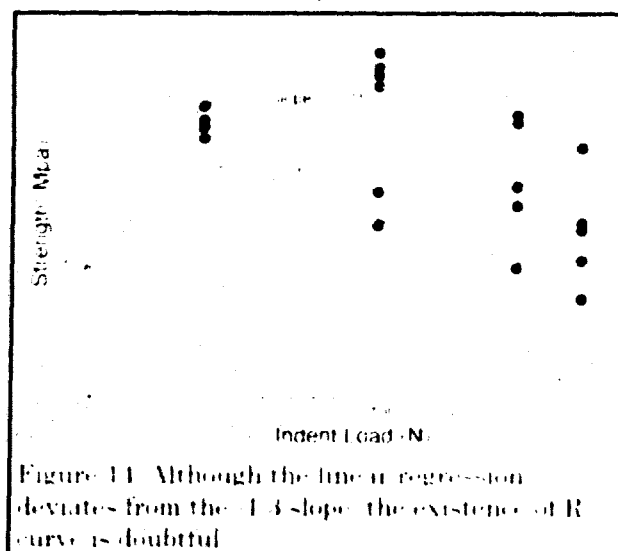


Figure 14 Although the linear regression deviates from the -1/3 slope, the existence of R curve is doubtful.

material was low after indentation. The low strength might be due to porosity. A large amount of microporosity formed during the high temperature post-HIP cycles. It appears that these conditions are too severe for the HIP silicon nitride. Grain size data was collected for several of these mixes after two hours at 2150 °C. The thickness distributions are shown in Figure 15. The final grain sizes are quite different for the various additive systems. The average grain size versus time is plotted for the binary rare earths and the yttria composition in Figure 16. Several factors may be influencing the differences in growth rate. Both rare earth mixtures had a slower grain growth rate. In addition, the rare earth mixture Er50YS with added silica had a slower grain growth rate than the ND50Y. The higher silica may retard the α to β transformation, because the nitrogen solubility decreases as the rare earth content decreases.

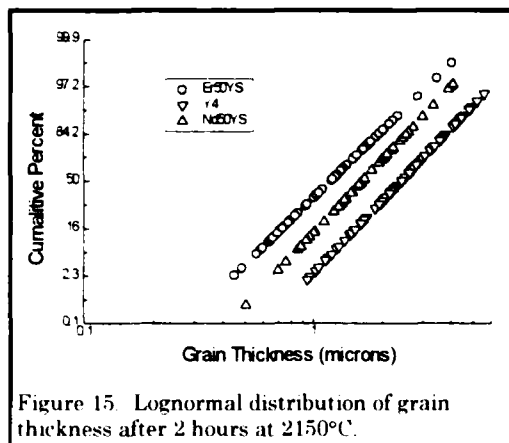


Figure 15. Lognormal distribution of grain thickness after 2 hours at 2150°C.

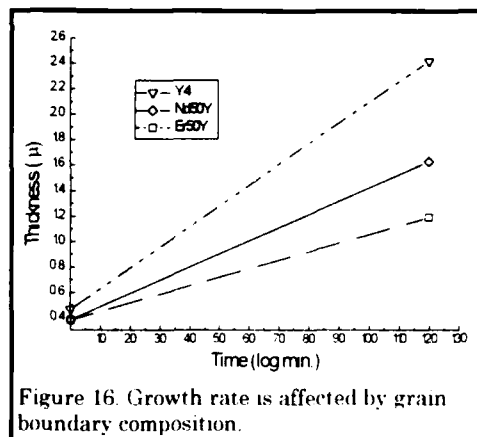


Figure 16. Growth rate is affected by grain boundary composition.

A third trial was done at 1840°C for an extended time of three hours with composition ErSm. Because the temperature was relatively low, significant grain coarsening and R-curve behavior were not expected. The plot of load versus strength is shown in Figure 17. The slope of -0.26 is less than -1/3, indicating crack length dependent toughness. Nd50YbS, one of the binary rare earths HIP at 1840 for 60 minutes, is included in Figure 17 for comparison. Nd50YbS does not exhibit crack length dependent toughness. Toughness as a function of crack length for ErSm was estimated using the method described by Krause.⁹ Improved techniques are available,⁶ but these were beyond the scope of the present work. The crack dependent toughness

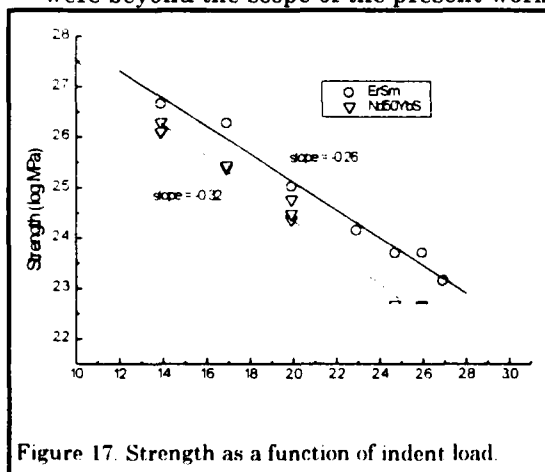


Figure 17. Strength as a function of indent load.

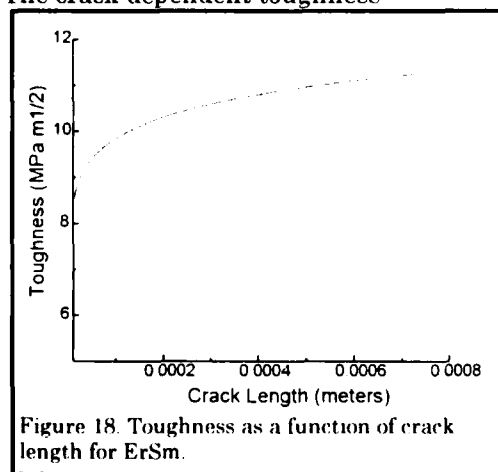


Figure 18. Toughness as a function of crack length for ErSm.

for ErSm is shown in Figure 18. The maximum toughness approaches 11 MPa m^{1/2} at crack lengths of 600 microns to 800 microns. The grain distribution of ErSm after a total of 4 hours at 1840°C is compared to

La40YbS and Y4SA densified at 1840°C for 60 minutes in Figure 19. The ErSm grain distribution is wider, based on the reduced slope of the grain distribution in Figure 19. The ErSm has a significant population of grains with a thickness of 1 micron or greater, which would favor toughening by grain bridging mechanisms. The apparent aspect ratio is compared to La40YbS in Figure 20. A significant number of grains with a thickness of 1 micron or greater developed modest aspect ratios in ErSm. Fine grains with high aspect ratios were also observed. The microstructural changes observed support the presence of R-curve behavior in ErSm.

A second cycle was run at 1840°C for five hours with compositions SmBS, NdYb, YbBS and ErSm. Including the original HIP densification cycle, the total time at 1840°C was 6 hours. Based on the dependence of strength on indent load, both rare earth mixtures exhibited R-curve behavior. Only the samaria composition with β seeds exhibited R-curve. Figure 21 shows the dependence of strength on indent load. The dependence of toughness on crack length for NdYb and ErSm after postHIP HIP is shown in Figure 22. The maximum toughness is slightly lower than observed with the 3 hour soak in Figure 18. The reduced dependence of toughness on crack length is expected to be due to continuing grain coarsening and loss of the fine high aspect ratio grains. Microstructure analysis of these materials was not completed.

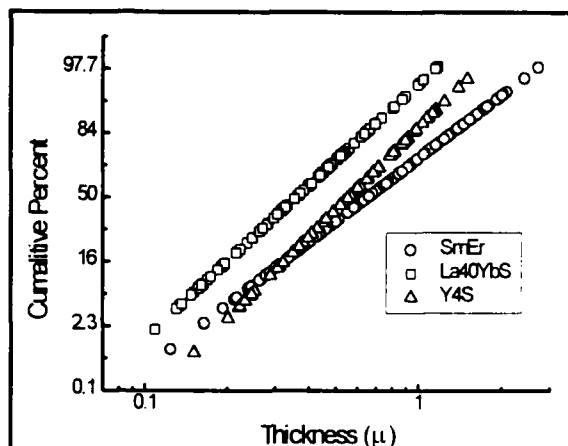


Figure 19. The grain distribution of ErSm after an extended time at 1840°C is broader than the other two materials HIPed at 1840°C for 60 minutes.

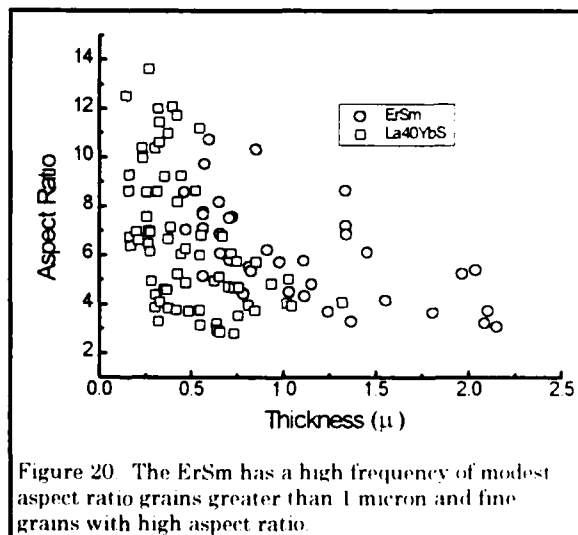


Figure 20. The ErSm has a high frequency of modest aspect ratio grains greater than 1 micron and fine grains with high aspect ratio.

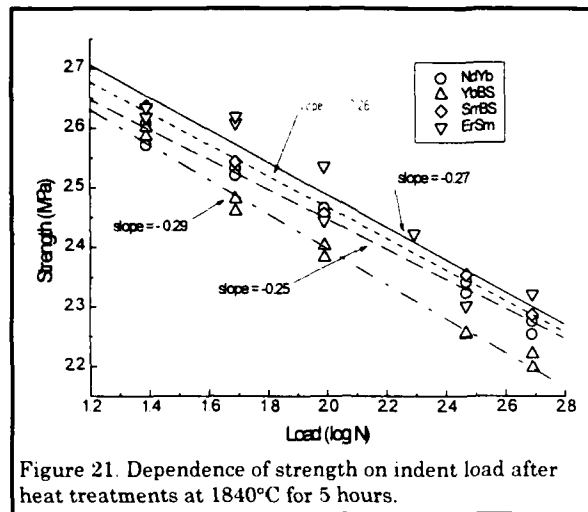


Figure 21. Dependence of strength on indent load after heat treatments at 1840°C for 5 hours.

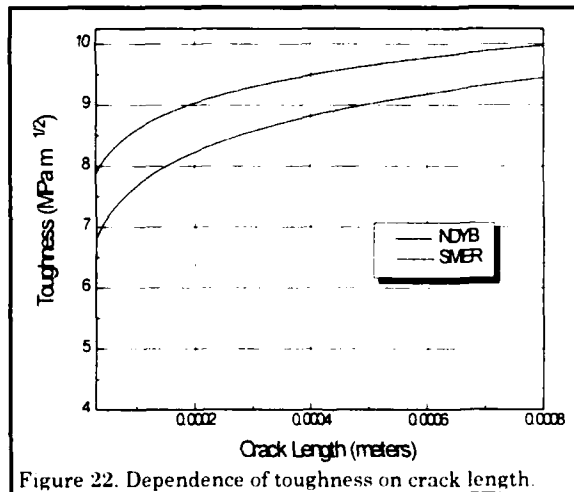


Figure 22. Dependence of toughness on crack length.

An alternative method to physically adding seeds to the powder is beta nuclei formation during thermal treatments. Two attempts were made at pre-HIP sintering tile at 2000°C for 30 minutes. Characterization of the materials after the pre-HIP sinter cycle was not completed. Density after sintering was less than 85%. Additionally, pre-HIP sinter conditions were not evaluated. The tile were then HIPed at 1840°C for 60 minutes. The first trial successfully densified the tile, but the second trial did not. Loss of encapsulation is the expected cause. The presintered tile are probably more

difficult to densify as they take longer to reach closed porosity, and the chance of encapsulation failure is higher. The materials that did densify were tested for R-curve. Two compositions contained beta seeds, and three did not. The composition with 10 w/o seeds did not exhibit R-curve. Four of the compositions did exhibit R-curve behavior, as shown in Figure 23. During the pre-HIP sinter cycle, appreciable transformation is expected

along with grain coarsening. The average grain size after the pre-HIP sinter and HIP is expected to be larger than a silicon nitride that was HIPed only. The average aspect ratio is probably lower than the HIPed materials. The pre-HIP sinter step at 2000°C probably coarsened the microstructure sufficiently to eliminate the fine high aspect beta grains observed after densification in the HIP. The microstructure was not characterized to determine whether these changes could be observed.

3.4 HIGH TEMPERATURE BEHAVIOR

A secondary objective of the program was to maintain the high temperature properties of the silicon nitride with increased toughness. The creep behavior would be influenced by the glass composition and grain size. The high temperature strength and creep behavior of yttria densified silicon nitride and samaria-ytterbia densified silicon nitride were compared.

The high temperature strengths of the samaria-ytterbia densified silicon nitrides exhibited a minimum at a rare earth to silica ratio of 0.17, as seen in Figure 24. The strengths were low as compared to NT154 which averages 80 to 90 ksi at 1370°C. The mixed rare earths did not show any evidence that crystallization of the intergranular phase had occurred during HIP. In NT154, some fraction of the intergranular phase crystallizes during the HIP cycle. The difference in the extent of crystallization may account for the lower strength of the samaria-ytterbia densified silicon nitride. The yttria-silica compositions, while stronger than the samaria-ytterbia, had strengths lower than NT154. The high temperature strength for the yttria-silica series is shown in Figure 25. The compositions prepared in this work have a lower surface area. NT154 has an additional process step that improves high temperature properties. This step was not followed in this program.

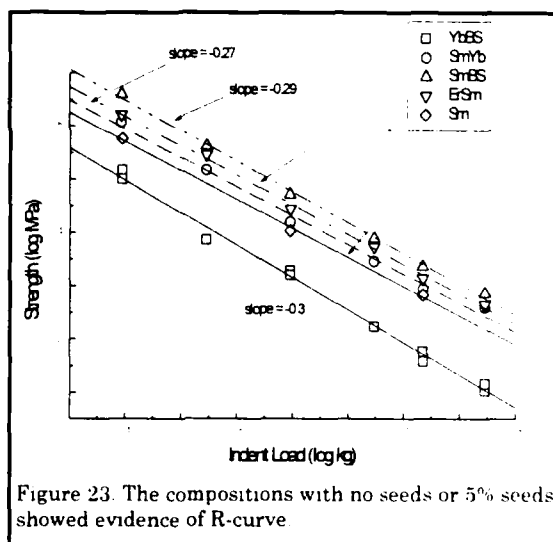


Figure 23. The compositions with no seeds or 5% seeds showed evidence of R-curve.

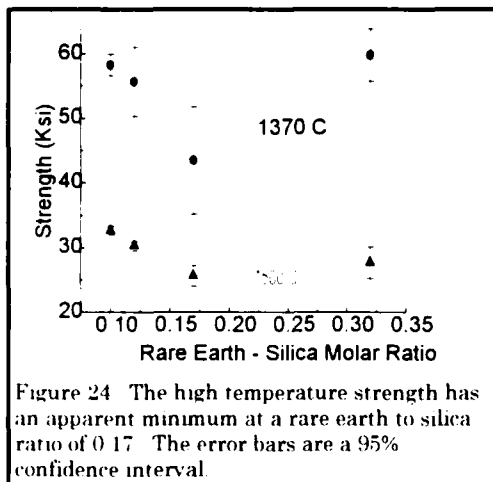


Figure 24 The high temperature strength has an apparent minimum at a rare earth to silica ratio of 0.17. The error bars are a 95% confidence interval.

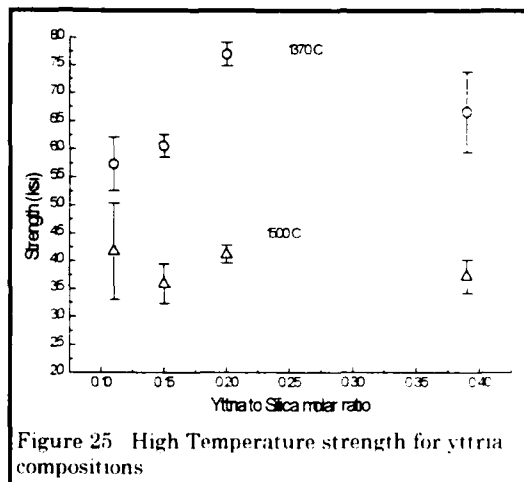


Figure 25 High Temperature strength for yttria compositions

The difference in intergranular crystallization should be expected to affect the relative creep behavior of the mixed rare earth densified silicon nitride. Compressive creep tests were conducted at 1370°C. All samples exhibited primary creep, followed by a secondary or steady state creep regime. Figure 26 is an example of a strain-time plot. The plot shows the strain with time between each adjacent flag; 1 to 2, 2 to 3 and 3 to 4. The overall strain, shown between Flags 1 to 4, would be expected to fall at a value intermediate to the other three measurements. All tests were suspended between 100 to 200 hours. The steady state creep rates for the samaria-ytterbia and the yttria series are compared in Figure 27. The steady state creep rates were very similar until the highest silica content. The samaria-ytterbia at the highest silica content has a creep rate much higher than the samaria-ytterbia with lower silica, or any of the yttria-silica densified silicon nitride. Additional testing must be done to confirm these trends, but the important conclusion is that the creep rate is not drastically increased by the alternate rare earths.

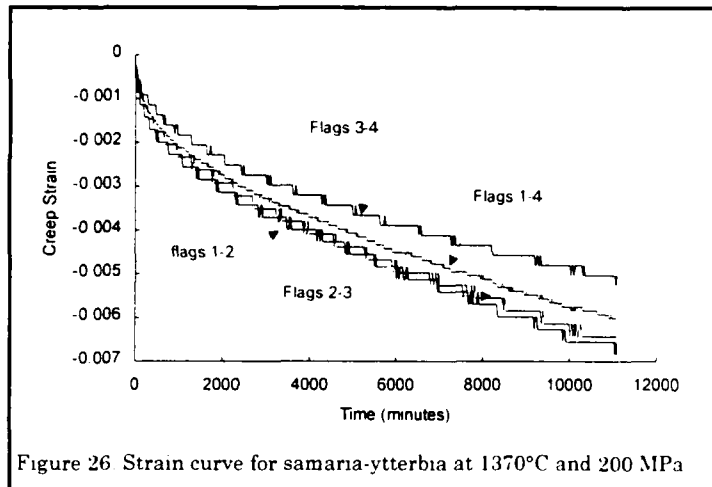


Figure 26 Strain curve for samaria-ytterbia at 1370°C and 200 MPa

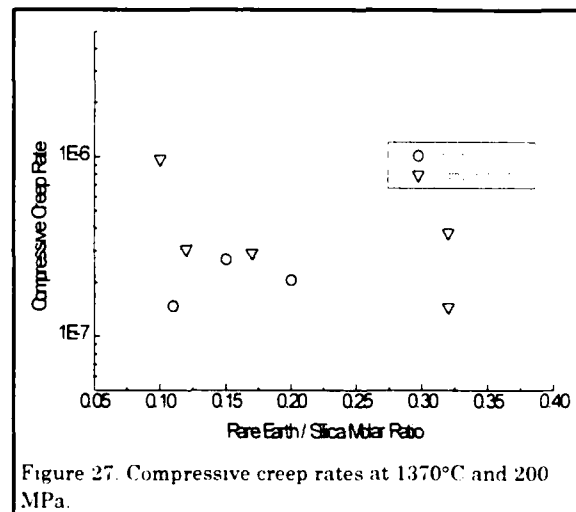


Figure 27. Compressive creep rates at 1370°C and 200 MPa.

Many studies have shown the formation of cavities during the tensile creep of HIP silicon nitride. Cavities formed during tensile creep tests were readily visible in the SEM. Figure 28 shows the formation of similar cavities in the silicon nitride with yttria at 1370°C and 200 MPa.

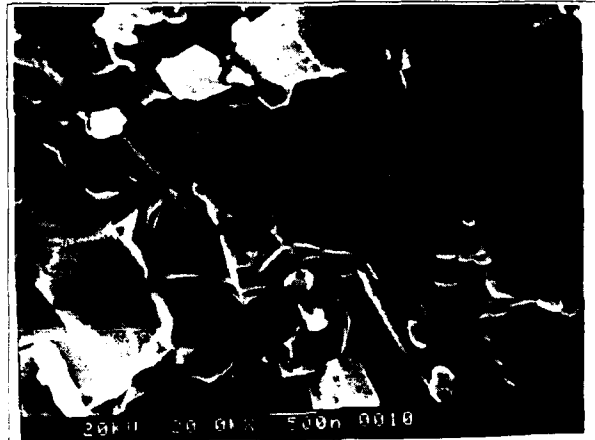


Figure 28. Cavitation on two grain boundaries occurs in compressive creep.

4.0 CONCLUSIONS

During the first year of the contract, several factors improving the fracture toughness were demonstrated. The use of binary rare earths resulted in a finer grain size and higher aspect ratio microstructure. This yielded an increased short crack toughness through crack deflection mechanisms. Crack bridging mechanisms were needed to achieve the contract fracture toughness goals.

Two densification approaches exhibited R curve behavior. Extended soaks at 1840°C produced toughness of approximately $10 \text{ MPa m}^{1/2}$ with relatively short crack lengths as compared to some GPS materials. The second approach presintered the tile at 2000°C for 30 minutes, then HIPed them at 1840°C for 60 minutes. These tiles also exhibited R Curve. The presinter step probably enabled the formation of large β nuclei. These nuclei could then grow during HIP to form grains with modest aspect ratios and diameters above 1 micron. The development completed during the first year of the program demonstrated that a HIP material with superior creep resistance, as well as high toughness, could be developed. The R-curve behavior observed occurs over a relatively short crack length. The microstructure does not have extremely large grains, and would be expected to have high strength. This would be an advantage over GPS materials, which reach maximum toughness at extremely long crack lengths.

5.0 REFERENCES

1. M.Mitomo, "Toughening of Silicon Nitride Ceramics by Microstructure Control", Proceedings of the 1st International Symposium on the Science of Engineering Ceramics.
2. K.Matsuhiro and T.Takahashi, "The Effect of Grain Size on the Toughness of Sintered Si_3N_4 ", Proceedings of the 13th Annual Conference on Composites and Advanced Ceramics.
3. M.Mitomo and K.Mizuno, "Sintering Behavior of Si_3N_4 with Y_2O_3 and Al_2O_3 Addition", *Yogyo-Kyokai* 94 [1] 1986.
4. P. F. Becher, H.T.Lin, S.L.Hwang, M.J.Huffmann, I-W. Chen, "The Influence of Microstructure on the Mechanical Behavior of Silicon Nitride Ceramics", in *Silicon Nitride Ceramics Scientific and Technological Advances*, MRS Vol 287, 1993.
5. D. Sordlett, "Densification and Microstructural Development of Two Si_3N_4 Alloys During Hot Isostatic Pressing", *Journal of the European Cer. Soc.* 10 (1992) 283-289.
6. O-H. Kwon and G. Messing, "HIP of Liquid Phase Sintered Ceramic Composites", in *Tailoring Multiphase Ceramics and Composite Ceramics*, pp. 41-55, Plenum, New York (1986).
7. D.Wittmer, D.Doshi, T.Paulson, "Development of $\beta\text{-Si}_3\text{N}_4$ for Self-Reinforced Composites".
8. K.T.Faber and A.G.Evans, "Crack Deflection Processes - I Theory", *Acta Metall.* Vol 31, No. 4 pp. 565-76 (1983).
9. R.F.Krause, "Rising Fracture Toughness from the Bending Strength of Indented Alumina Beams", *J.Am.Cer.Soc.* 71 [5] 338-43 (1988).

DISTRIBUTION LIST

| No. of Copies | To |
|------------------|--|
| 1 | Office of the Under Secretary of Defense for Research and Engineering, The Pentagon, Washington, DC 20301 |
| | Director, U.S. Army Research Laboratory, 2800 Powder Mill Road, Adelphi, MD 20783-1197 |
| 1 | ATTN: AMSRL-OP-CI-AD, Technical Publishing Branch |
| 1 | AMSRL-OP-CI-AD, Records Management Administrator |
| | Commander, Defense Technical Information Center, Cameron Station, Building 5, 5010 Duke Street, Alexandria, VA 23304-6145 |
| 2 | ATTN: DTIC-FDAC |
| 1 | MIA/CINDAS, Purdue University, 2595 Yeager Road, West Lafayette, IN 47905 |
| | Commander, Army Research Office, P.O. Box 12211, Research Triangle Park, NC 27709-2211 |
| 1 | ATTN: Information Processing Office |
| | Commander, U.S. Army Materiel Command, 5001 Eisenhower Avenue, Alexandria, VA 22333 |
| 1 | ATTN: AMCSCI |
| | Commander, U.S. Army Materiel Systems Analysis Activity, Aberdeen Proving Ground, MD 21005 |
| 1 | ATTN: AMXS-MP, H. Cohen |
| | Commander, U.S. Army Missile Command, Redstone Arsenal, AL 35809 |
| 1 | ATTN: AMSMI-RD-CS-R/Doc |
| | Commander, U.S. Army Armament, Munitions and Chemical Command, Dover, NJ 07801 |
| 2 | ATTN: Technical Library |
| | Commander, U.S. Army Natick Research, Development and Engineering Center, Natick, MA 01760-5010 |
| 1 | ATTN: Technical Library |
| | Commander, U.S. Army Satellite Communications Agency, Fort Monmouth, NJ 07703 |
| 1 | ATTN: Technical Document Center |
| | Commander, U.S. Army Tank-Automotive Command, Warren, MI 48397-5000 |
| 1 | ATTN: AMSTA-ZSK |
| 1 | AMSTA-TSL, Technical Library |
| | Commander, White Sands Missile Range, NM 88002 |
| 1 | ATTN: STEWS-WS-VT |
| | President, Airborne, Electronics and Special Warfare Board, Fort Bragg, NC 28307 |
| 1 | ATTN: Library |
| | Director, U.S. Army Research Laboratory, Weapons Technology, Aberdeen Proving Ground, MD 21005-5066 |
| 1 | ATTN: AMSRL-WT |

| No. of Copies | To |
|------------------|--|
| 1 | Commander, Dugway Proving Ground, UT 84022 ATTN: Technical Library, Technical Information Division |
| 1 | Commander, U.S. Army Research Laboratory, 2800 Powder Mill Road, Adelphi, MD 20783 ATTN: AMSRL-SS |
| 1 | Director, Benet Weapons Laboratory, LCWSL, USA AMCCOM, Watervliet, NY 12189 ATTN: AMSMC-LCB-TL |
| 1 | AMSMC-LCB-R |
| 1 | AMSMC-LCB-RM |
| 1 | AMSMC-LCB-RP |
| 3 | Commander, U.S. Army Foreign Science and Technology Center, 220 7th Street, N.E., Charlottesville, VA 22901-5396 ATTN: AIFRTC, Applied Technologies Branch, Gerald Schlesinger |
| 1 | Commander, U.S. Army Aeromedical Research Unit, P.O. Box 577, Fort Rucker, AL 36360 ATTN: Technical Library |
| 1 | U.S. Army Aviation Training Library, Fort Rucker, AL 36360 ATTN: Building 5906-5907 |
| 1 | Commander, U.S. Army Agency for Aviation Safety, Fort Rucker, AL 36362 ATTN: Technical Library |
| 1 | Commander, Clarke Engineer School Library, 3202 Nebraska Ave., N, Fort Leonard Wood, MO 65473-5000 ATTN: Library |
| 1 | Commander, U.S. Army Engineer Waterways Experiment Station, P.O. Box 631, Vicksburg, MS 39180 ATTN: Research Center Library |
| 1 | Commandant, U.S. Army Quartermaster School, Fort Lee, VA 23801 ATTN: Quartermaster School Library |
| 2 | Naval Research Laboratory, Washington, DC 20375 ATTN: Dr. G. R. Yoder - Code 6384 |
| 1 | Chief of Naval Research, Arlington, VA 22217 ATTN: Code 471 |
| 1 | Commander, U.S. Air Force Wright Research & Development Center, Wright-Patterson Air Force Base, OH 45433-6523 ATTN: WRDC/MLLP, M. Forney, Jr. |
| 1 | WRDC/MLBC, Mr. Stanley Schulman |
| 1 | U.S. Department of Commerce, National Institute of Standards and Technology, Gaithersburg, MD 20899 ATTN: Stephen M. Hsu, Chief, Ceramics Division, Institute for Materials Science and Engineering |

| No. of Copies | To |
|------------------|---|
| 1 | Committee on Marine Structures, Marine Board, National Research Council, 2101 Constitution Avenue, N.W., Washington, DC 20418 |
| 1 | Materials Sciences Corporation, Suite 250, 500 Office Center Drive, Fort Washington, PA 19034 |
| 1 | Charles Stark Draper Laboratory, 555 Technology Square, Cambridge, MA 02139 |
| | Wyman-Gordon Company, Worcester, MA 01601 |
| 1 | ATTN: Technical Library |
| | General Dynamics, Convair Aerospace Division, P.O. Box 748, Fort Worth, TX 76101 |
| 1 | ATTN: Mfg. Engineering Technical Library |
| | Plastics Technical Evaluation Center, PLASTEC, ARDEC, Bldg. 355N, Picatinny Arsenal, NJ 07806-5000 |
| 1 | ATTN: Harry Peibly |
| 1 | Department of the Army, Aerostructures Directorate, MS-266, U.S. Army Aviation R&T Activity - AVSCOM, Langley Research Center, Hampton, VA 23665-5225 |
| 1 | NASA - Langley Research Center, Hampton, VA 23665-5225 |
| | U.S. Army Vehicle Propulsion Directorate, NASA Lewis Research Center, 2100 Brookpark Road, Cleveland, OH 44135-3191 |
| 1 | ATTN: AMSRL-VP |
| | Director, Defense Intelligence Agency, Washington, DC 20340-6053 |
| 1 | ATTN: ODT-5A (Mr. Frank Jaeger) |
| | U.S. Army Communications and Electronics Command, Fort Monmouth, NJ 07703 |
| 1 | ATTN: Technical Library |
| | U.S. Army Research Laboratory, Electronic Power Sources Directorate, Fort Monmouth, NJ 07703 |
| 1 | ATTN: Technical Library |
| | Director, U.S. Army Research Laboratory, Watertown, MA 02172-0001 |
| 2 | ATTN: AMSRL-OP-CI-D, Technical Library |
| 1 | AMSRL-OP-CI-D, Visual Information Unit |
| 1 | AMSRL-OP-PR-WT |
| 6 | AMSRL-MA-MA, George Gazza COR |